Supporting Information for

Revealing EDL-Driven Reduction Mechanisms in Binary, Ternary, and Quaternary Fluorinated Electrolytes via an Integrated MD–DFT–ML Framework

Md Jamil Hossain,[†a] *Tilas Kabengele,*[†a,d] *Qisheng Wu,*[a] *Patrick J. Barry,*[e,f] *Mia S. Mishaan,*[e,h] *Shan Yan,*[f,g] *Xiao Tong,*[i] *Amy C. Marschilok,*[e,f,g,h] *Kenneth J. Takeuchi,*[e,f,g,h] *Esther S. Takeuchi,*[e,f,g,h] *Brenda M. Rubenstein,*[b,c,d] *and Yue Qi*[‡a]

[a] School of Engineering, Brown University, Providence, RI, USA, 02912

[b] Department of Physics, Brown University, Providence, RI, USA, 02912

[c] Data Science Institute, Brown University, Providence, RI, USA, 02912

[d] Department of Chemistry, Brown University, Providence, RI, USA, 02912

[e] Institute of Sustainability, Electrification, and Energy (I:SEE), Stony Brook University, Stony Brook, NY, USA, 11794

[f] Department of Chemistry, Stony Brook University, Stony Brook, NY, USA, 11794

[g] Interdisciplinary Science Department, Brookhaven National Laboratory, Upton, NY, USA, 11973

[h] Department of Materials Science and Chemical Engineering, Stony Brook University, Stony Brook, NY, USA, 11794

[i] Center for Functional Nanomaterials, Brookhaven National Laboratory, Upton, NY, USA, 11973

[†] These authors contributed equally to this work.

[‡] Author to whom correspondence should be addressed: yueqi@brown.edu

DFT calculations of reorganization energies and energy barriers for electron transfer reactions. Marcus theory was used to calculate the reduction reaction barriers, following [1,2]

$$\Delta G^{barrier} = \frac{\lambda}{4}\left[1 + \frac{\Delta G^{reaction}}{\lambda}\right]^2, \quad \text{(S-1)}$$

where $\Delta G^{reaction}$ is the reaction free energy and λ is the reorganization energy, containing the inner-shell λ_{inner} and bulk outer-shell λ_{outer} reorganization energies. Thus, total reorganization energy is

$$\lambda = \lambda_{inner} + \lambda_{outer}, \quad \text{(S-2)}$$

The inner reorganization energy λ_{inner} can be calculated using Nelson's four-point method.[3] From **Figure S1,** we define the DFT computed Gibbs free energy of oxidized species at its optimized geometry, the reduced species at the optimized oxidized geometry, the reduced species at the optimized reduced geometry, and oxidized species at the optimized reduced geometry as G_1, G_2, G_3, and G_4, respectively. $\Delta G^{reaction} = G_3 - G_1$, and the inner shell reorganization energy is

$$\lambda_{inner} = \frac{\lambda_1 + \lambda_2}{2} = \frac{G_2 - G_3 + G_4 - G_1}{2}, \quad \text{(S-3)}$$

The outer shell reorganization energy is calculated as

$$\lambda_{outer} = \frac{(\Delta e)^2}{8\pi\varepsilon_0}\left(\frac{1}{r} - \frac{1}{2D}\right)\left(\frac{1}{n^2} - \frac{1}{\varepsilon_s}\right), \quad \text{(S-4)}$$

where Δe is the transferred electron with a value of 1.6×10^{-19} C for one-electron transfer. ε_0 is the permittivity of the vacuum, 8.85×10^{-12} F/m, r is the radius of the molecule, assumed to be 5 Å for our calculations, D is the molecule-electrode distance assumed to be 5 Å for our calculations, n^2 is the optical dielectric constant, which is the square of refractive index of the solvent, n. n^2= 2. ε_s is the dielectric constant of the solvent; $\varepsilon_s = 7.2273$ for our ether and ester solvents.

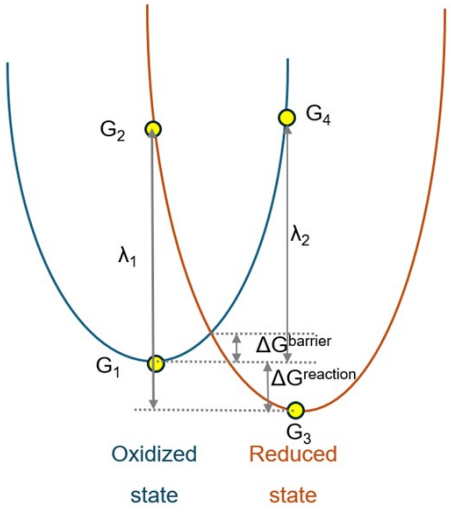

Figure S1: Diagram showing electron transfer reaction barrier and reaction energy.

Data and Statistical analyses of the EDL. In this work, the EDL is defined as the region within 13.0 Å from the surface of the negatively charged graphene electrode.[4] Species were considered to be located within the EDL if any of the atoms of the species were in the EDL. Since the Li^+ coordination can increase the reduction voltage of a solvent species dramatically,[5] we analyzed the statistics of the electrolyte in the EDL in terms of a) solvents/anions coordinated with Li^+ in the first solvation shell and b) free solvent/anions species (not coordinated to any Li^+). Following our recent publication,[6] we used the one-electron reduction-center based counting for the onset of electrolyte reduction reactions. This means, each Li^+-coordinated cluster was counted as one and the number of each Li^+-coordinated clusters type, N_i, sums to the total number of Li^+ ions, $N_{Li} = \sum_i N_i$. A cutoff of 2.8 Å was used to define the first solvation shell of Li^+ ion. Each free specie was counted as one and the number of each specie type, N_j, sums to the total number of free species, $N_f = \sum_j N_j$. Thus, the SEI formation probability for each Li^+-coordinated cluster, *i*, is $P_i = N_i/(N_{Li} + N_f)$, while the SEI formation probability for each free specie, *j*, is calculated as $P_j = N_j/(N_{Li} + N_f)$.

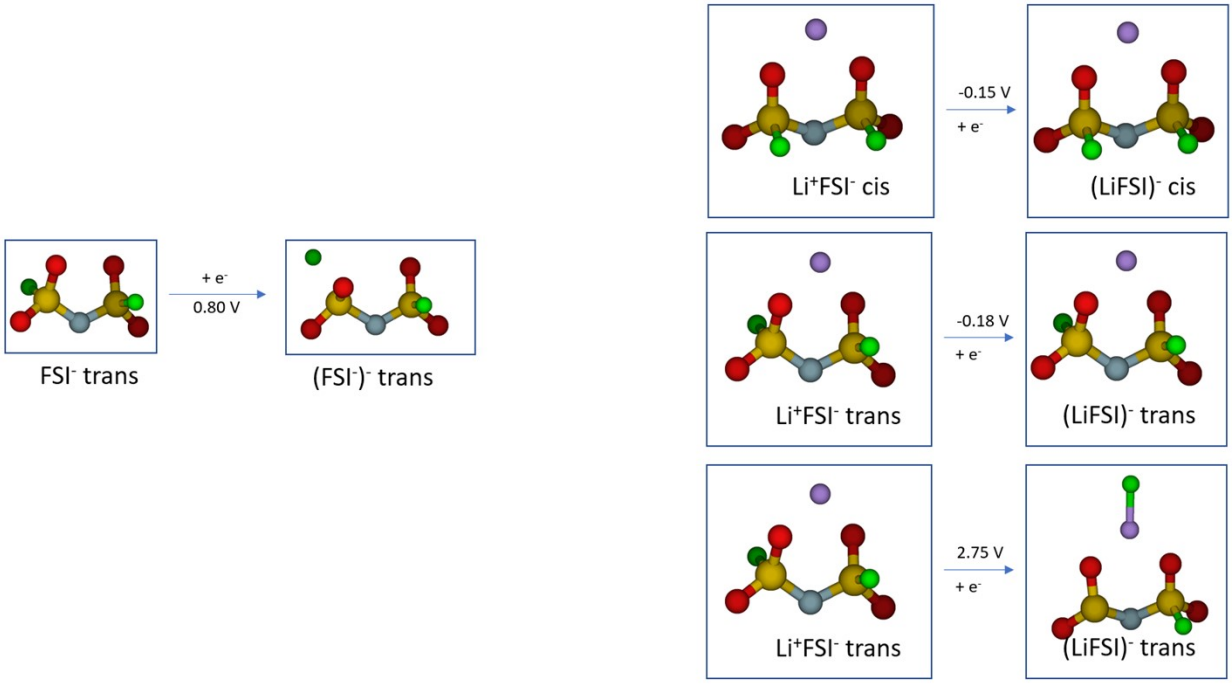

Figure S2: Reduction potential of FSI^- and Li^+FSI^- vs Li^+/Li.

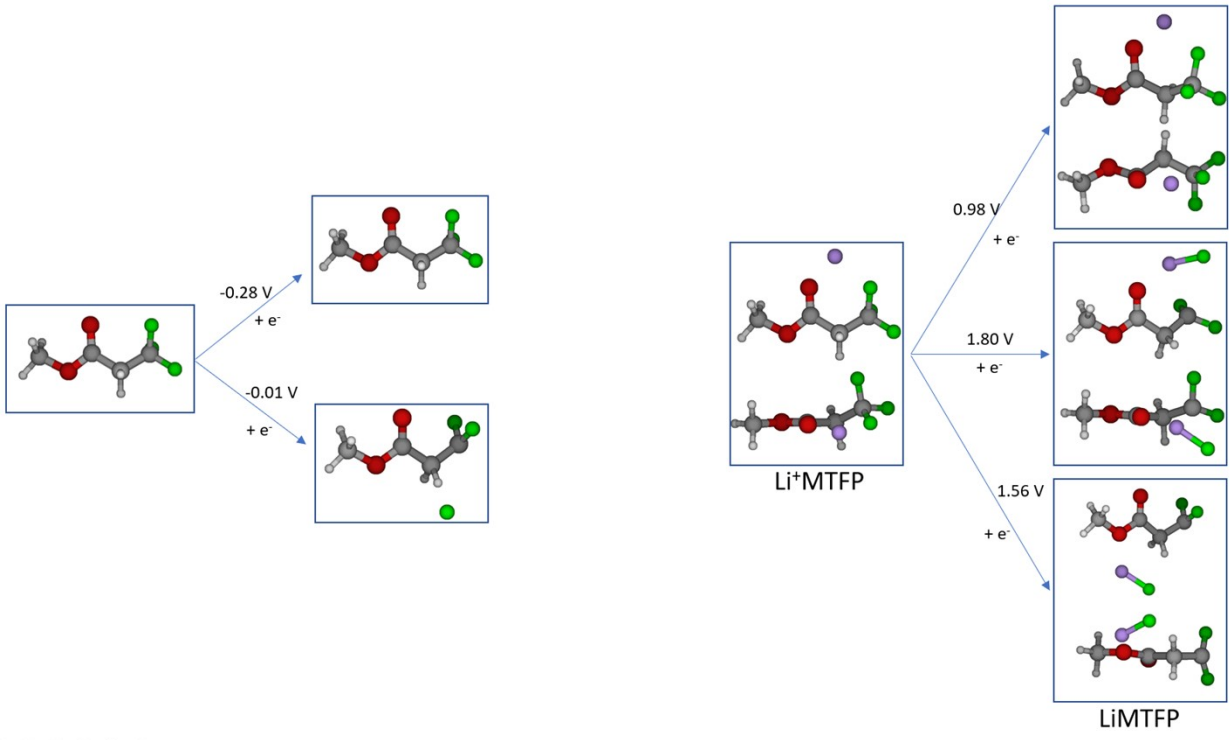

Figure S3: Reduction potential of MTFP and Li^+MTFP vs Li^+/Li.

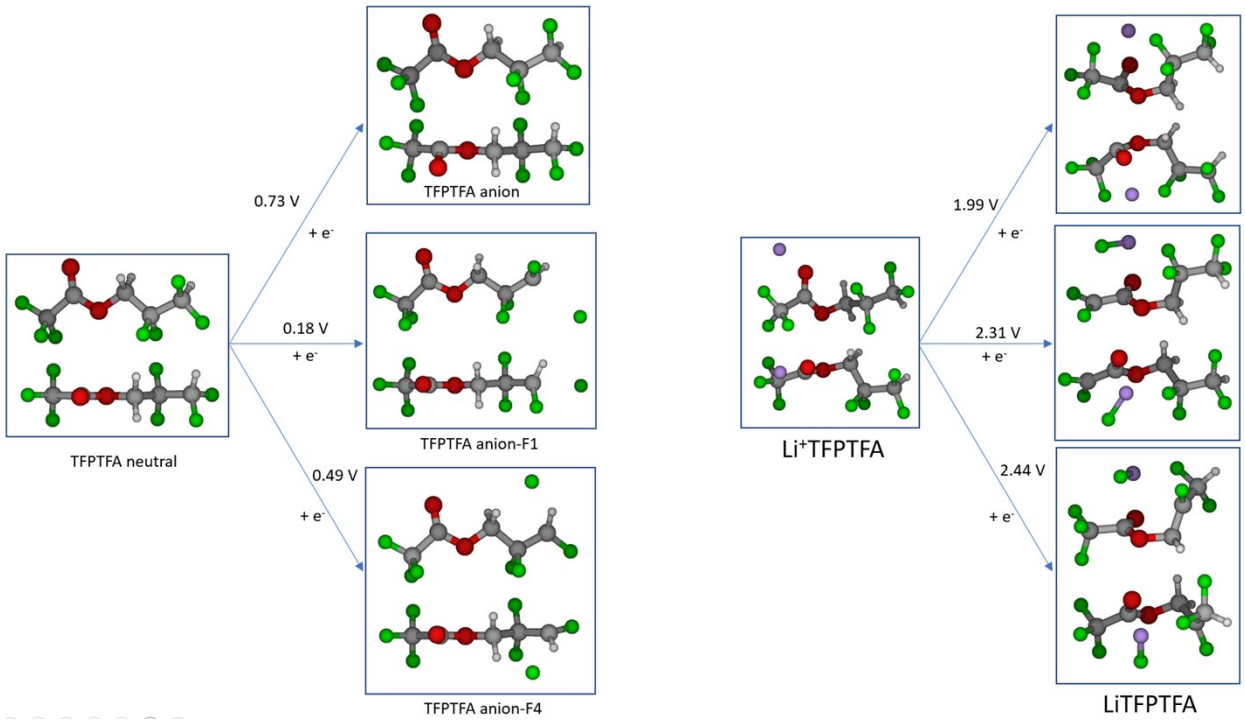

Figure S4: Reduction potential of TFPTFA and Li^+TFPTFA vs Li^+/Li.

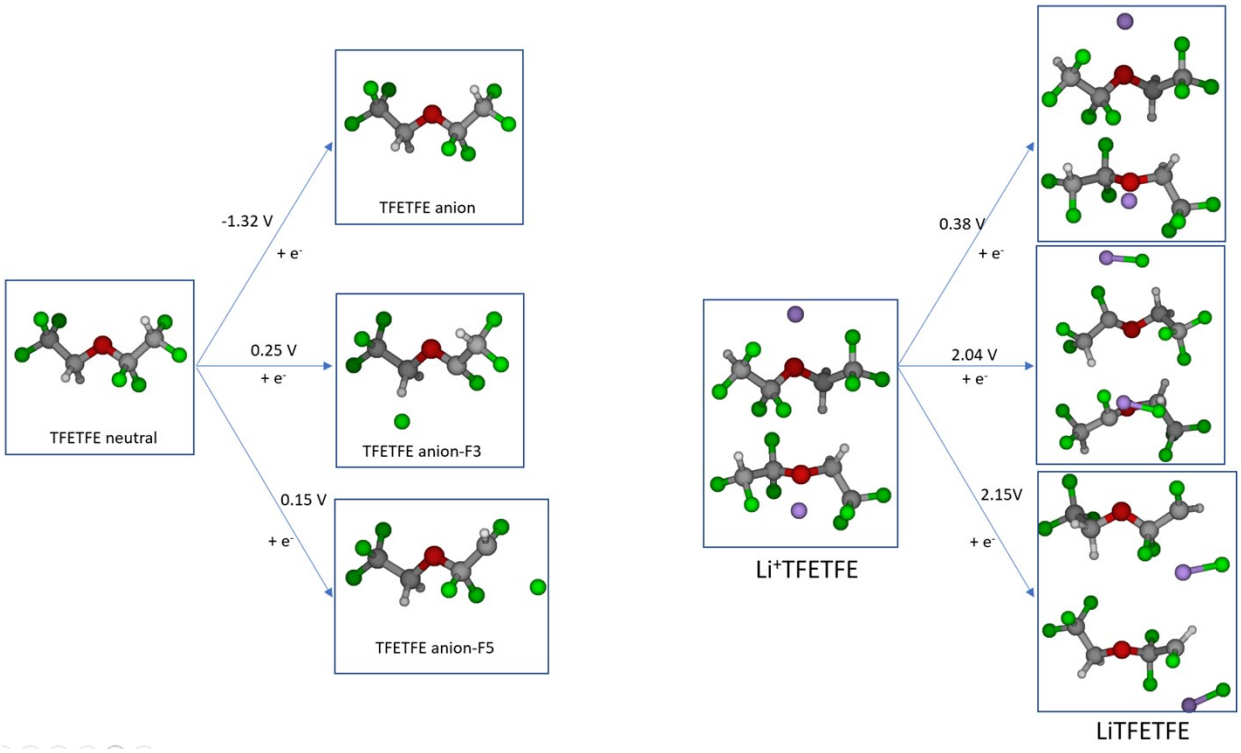

Figure S5: Reduction potential of TFETFE and Li^+TFETFE vs Li^+/Li.

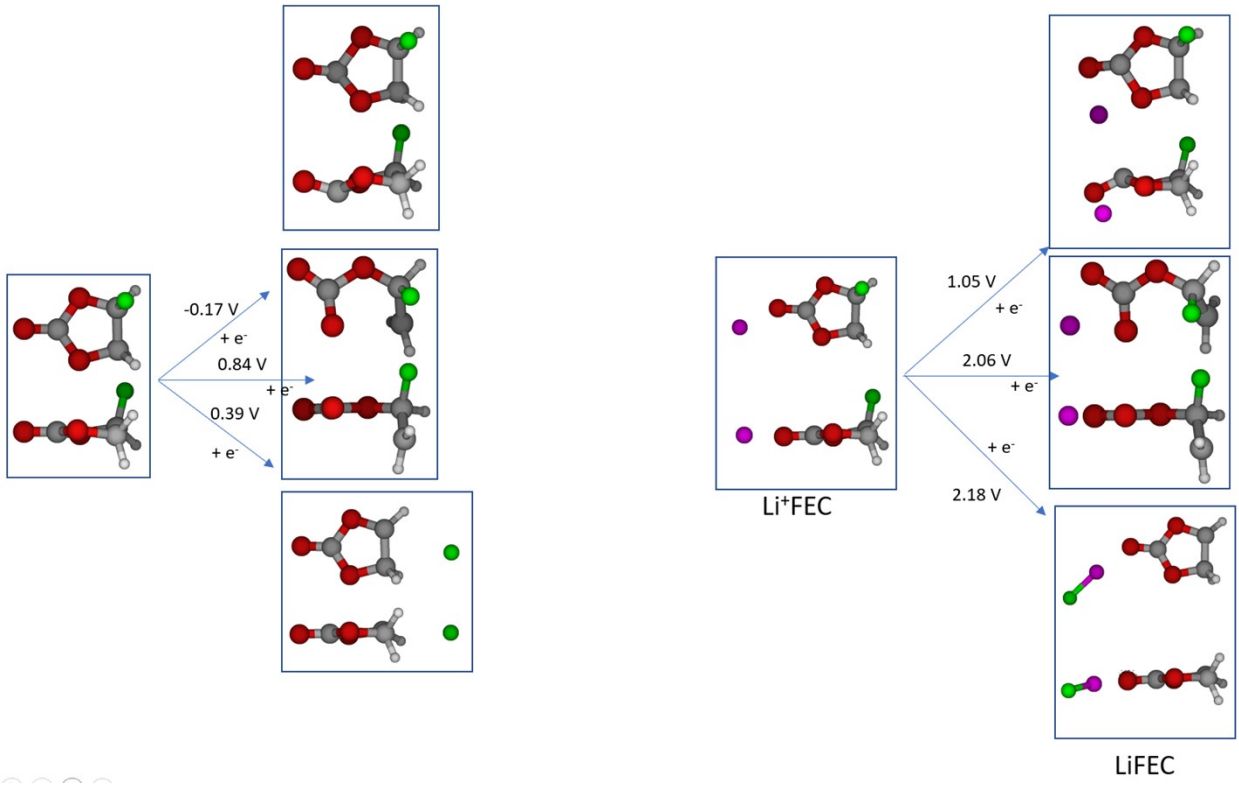

Figure S6: Reduction potential of FEC and Li^+FEC vs Li^+/Li.

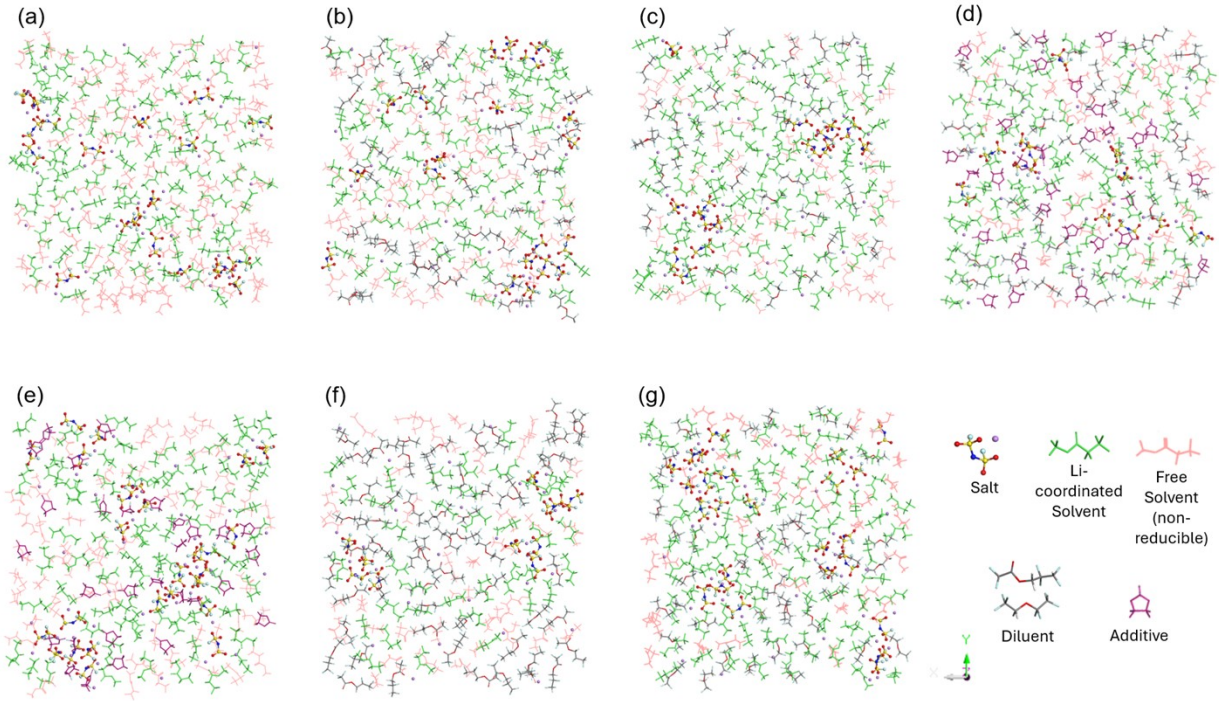

Figure S7: Top view of EDL structures adjacent to negatively charged electrode for (a) E1, (b) E2; (c) E4; (d) E7; (e) E6; (f) E3; and (g) E5.

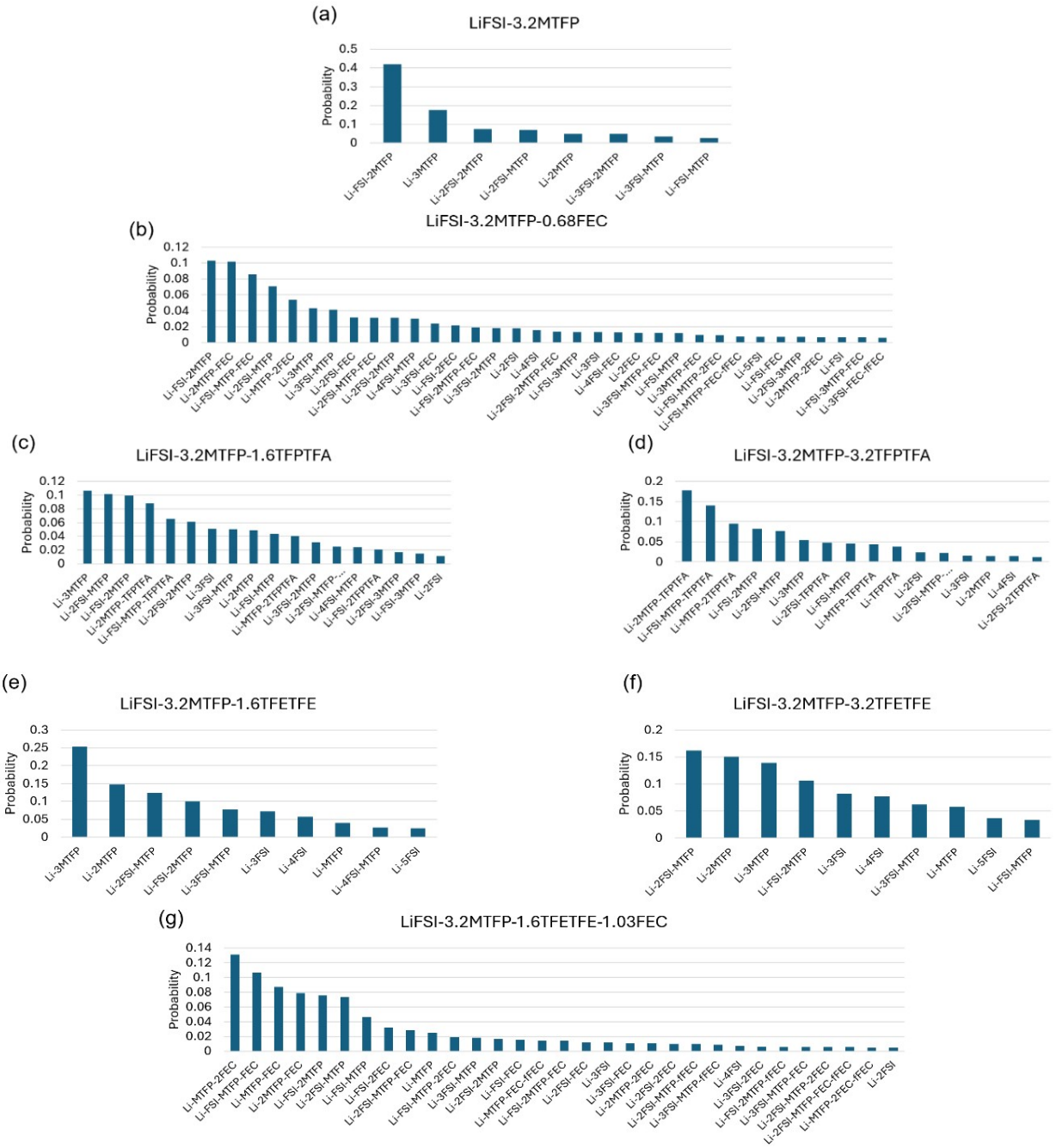

Figure S8: Probability distribution of various Li^+ centric first solvation shells in the EDL of electrolytes (a) E1; (b) E6; (c) E2; (d) E3; (e) E4; (f) E5; and (g) E7.

Train by Component (TBC): The model begins by learning patterns from simple, interpretable structures in P, and is then trained iteratively from E1 to E6, following the same progression as in the Training by Electrolyte (TBE) protocol in Figure 5.

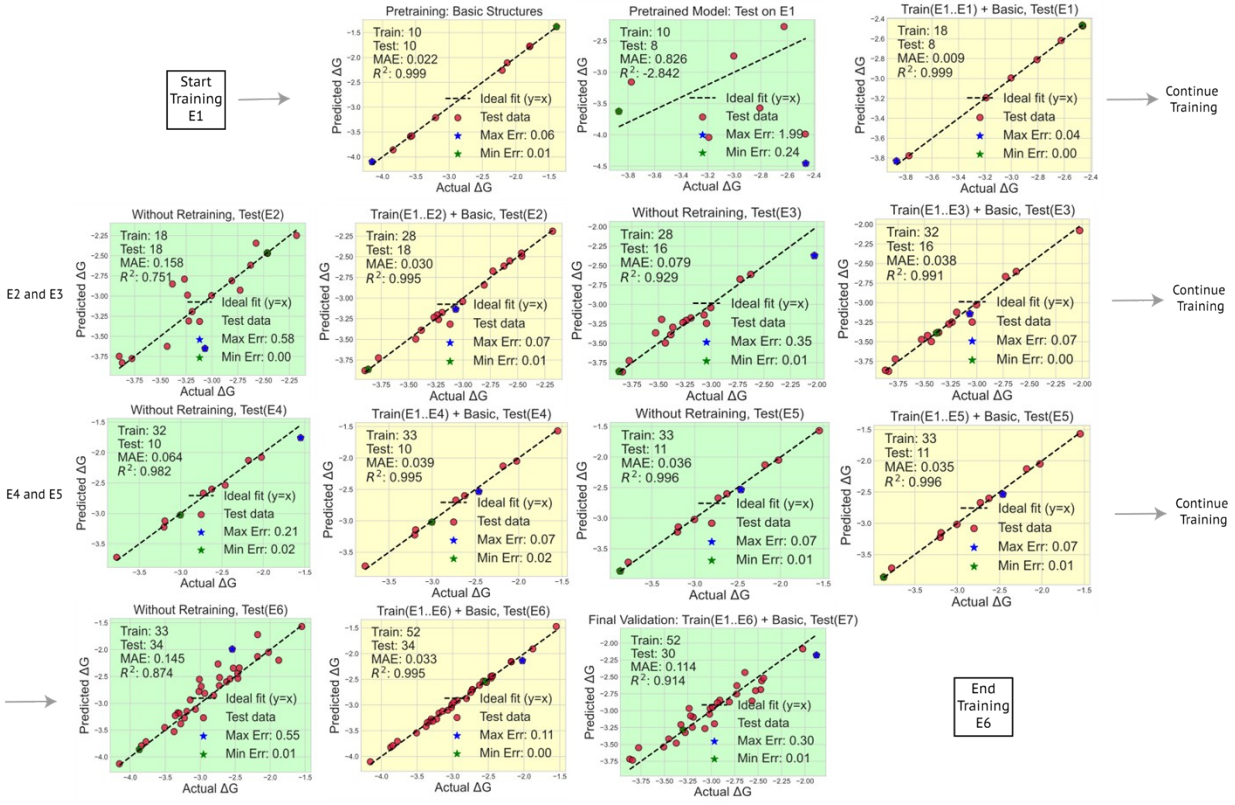

Figure S9: Iterative steps of the Train by Components protocol. The ML model was first pretrained on basic structures and Li^+-coordinated pairs, followed by electrolyte-specific training and final validation on E7. Final validation on E7 demonstrates the impact of cumulative chemical complexity on model generalization.

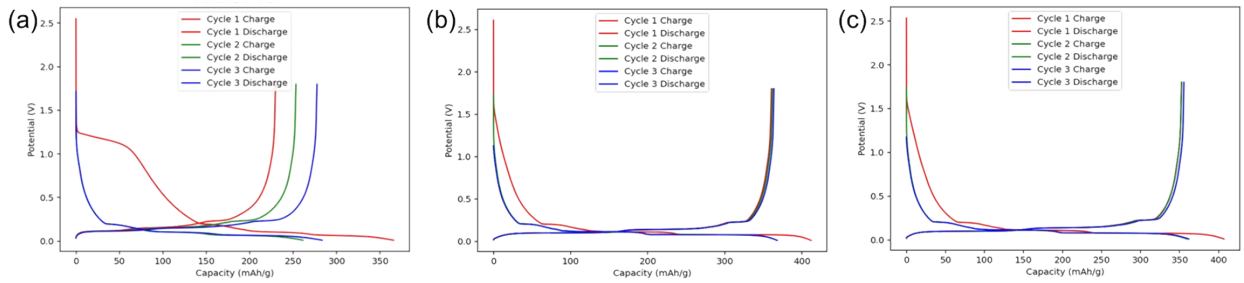

Figure S10: Voltage curves during galvanostatic cycling at C/10 for lithium/graphite cells containing (a) E1, (b) E6 and (c) E7 electrolytes.

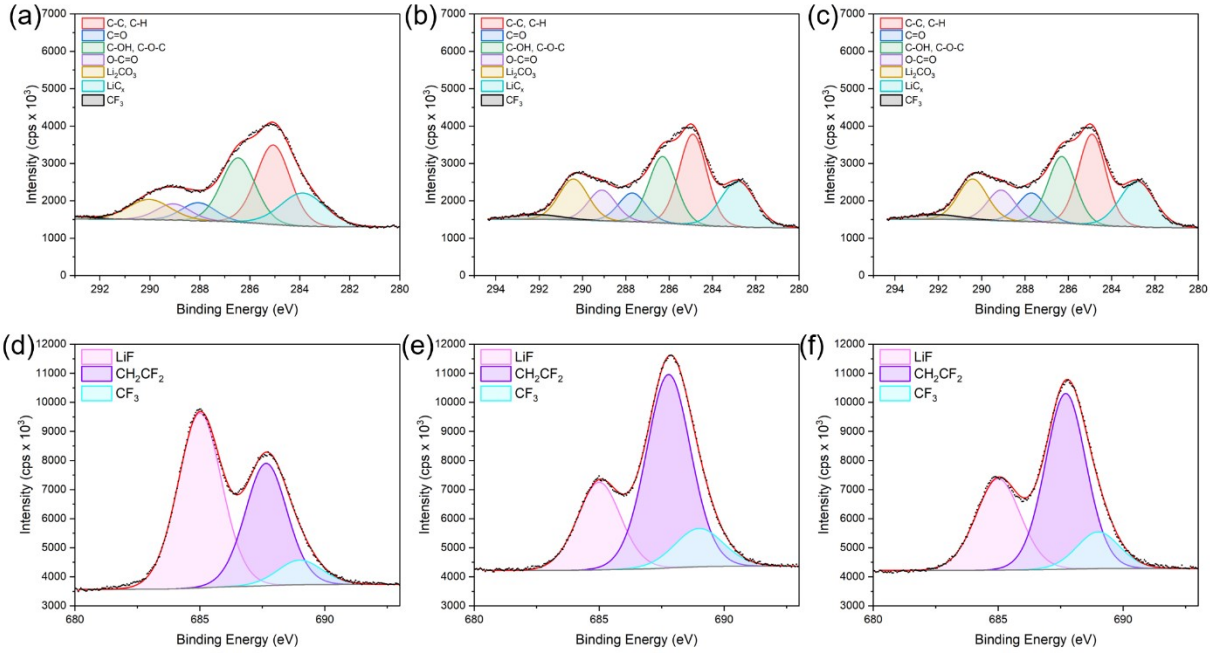

Figure S11: X-ray photoelectron spectroscopy (XPS) data from graphite electrodes recovered from lithium/graphite cells containing (a) E1, (b) E6 and (c) E7 electrolytes.

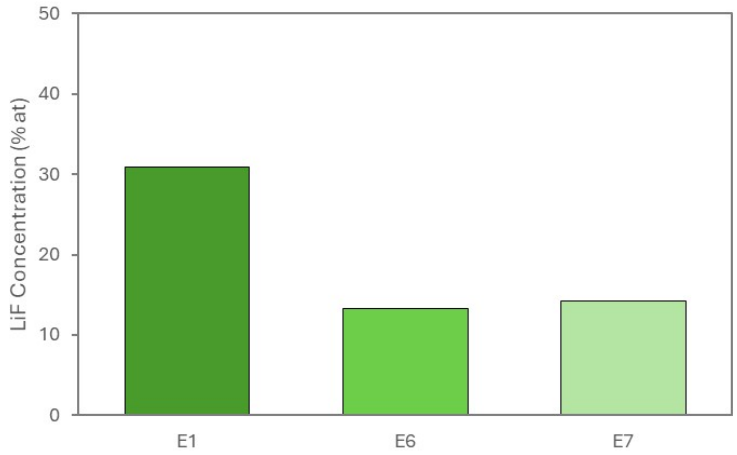

Figure S12: Atomic percent composition of LiF (as a percentage of total composition) from X-ray photoelectron spectroscopy (XPS) data from graphite electrodes recovered from lithium/graphite cells containing E1, E6 and E7 electrolytes.

Table S1: Average reduction potential* (V) vs Li^+/Li of the EDL structures of the different electrolytes studied.

Electrolytes		DFT reduction potential (V) vs Li^+/Li	
		inner adsorbed layer (0-5 Å)	Total EDL (0-13 Å)
E1	LiFSI-3.2MTFP	1.85	0.82
E2	LiFSI-3.2MTFP-1.6TFPTFA	1.65	0.64
E3	LiFSI-3.2MTFP-3.2TFPTFA	1.67	0.51
E4	LiFSI-3.2MTFP-1.6TFETFE	1.14	0.51
E5	LiFSI-3.2MTFP-3.2TFETFE	1.14	0.59
E6	LiFSI-3.2MTFP-0.68FEC	1.50	0.80
E7	LiFSI-3.2MTFP-1.6TFETFE-1.03FEC	1.29	0.62

*Assuming that every species in the EDL—both Li^+-centric solvation clusters and free species—has the same likelihood of capturing an electron, the overall average reduction potential is determined by summing the products of each species' occurrence probability and its respective reduction potential vs. Li^+/Li.

Table S2: Model transferability performance during iterative testing. The model is sequentially trained on progressively larger subsets of electrolyte data (denoted D_i), and tested on the next unseen electrolyte. Performance is reported using Mean Absolute Error (MAE) and coefficient of determination (R^2).

Train → Test	Train by Components MAE	Train by Components R^2	Train by Electrolytes MAE	Train by Electrolytes R^2
P → E1	0.826	-2.842	N/A	N/A
D_1 → E2	0.158	0.751	0.207	0.659
D_2 → E3	0.079	0.929	0.083	0.890
D_3 → E4	0.064	0.982	0.037	0.990
D_4 → E5	0.036	0.996	0.026	0.998
D_5 → E6	0.145	0.874	0.176	0.798
D_6 → E7	0.114	0.914	0.113	0.911

References

1. Marcus, R. A. Transfer reactions in chemistry. Theory and experiment. *Pure and applied chemistry* 69, 13–30 (1997).
2. Spotte-Smith, E. W. C. *et al.* Toward a Mechanistic Model of Solid-Electrolyte Interphase Formation and Evolution in Lithium-Ion Batteries. *ACS Energy Lett* 7, 1446–1453 (2022).
3. Nelsen, S. F., Blackstock, S. C. & Kim, Y. Estimation of inner shell Marcus terms for amino nitrogen compounds by molecular orbital calculations. *J Am Chem Soc* 109, 677–682 (1987).
4. Abbott, J. W. & Hanke, F. Kinetically Corrected Monte Carlo–Molecular Dynamics Simulations of Solid Electrolyte Interphase Growth. *J Chem Theory Comput* 18, 925–934 (2022).
5. Borodin, O., Olguin, M., Spear, C. E., Leiter, K. W. & Knap, J. Towards high throughput screening of electrochemical stability of battery electrolytes. *Nanotechnology* 26, 354003 (2015).
6. Wu, Q., McDowell, M. T. & Qi, Y. Effect of the Electric Double Layer (EDL) in Multicomponent Electrolyte Reduction and Solid Electrolyte Interphase (SEI) Formation in Lithium Batteries. *J Am Chem Soc* 145, 2473–2484 (2023).